

Synthesis, anticancer evaluation and docking study of vadimezan derivatives with carboxyl substitution†

Cite this: *Med. Chem. Commun.*, 2014, 5, 512

Shi-Jie Zhang,^a Zhi-Shan Ding,^b Fu-Sheng Jiang,^b Qiu-Fu Ge,^c Dian-Wu Guo,^c Hai-Bo Li^d and Wei-Xiao Hu^{*e}

A series of xanthone analogues modified from vadimezan **6** with carboxyl substitution were synthesized as esters, amides, arylidene hydrazides, diacylhydrazides and acyl thiosemicarbazides, and their structures were confirmed by IR, ¹H NMR, MS, HRMS or elemental analysis. The *in vitro* anticancer activities were evaluated by the MTT method. It was found that compounds **8f**, **8g** and **10e** were effective against A549 with an IC₅₀ at 10.8 μM, 9.4 μM and 11.5 μM respectively, and that **8e** was effective against HL-60 with an IC₅₀ at 4.6 μM. Compounds **8f–h** showed a significant inhibitory effect on HUVEC growth and migration *in vitro*, among which **8h** inhibited HUVEC growth with an IC₅₀ at 6.4 μM and HUVEC migration by 67.6% and 89.7% at 2.5 μg mL⁻¹ and 10 μg mL⁻¹ respectively. More spectacularly, docking study indicated that compound **8h** might target the ATP binding site of VEGFR2. In addition, compounds **8a**, **8f–h** exhibited moderate *in vivo* antitumor efficacy against the S180 xenograft in ICR mice by 22.4–29.6% tumor weight inhibition.

Received 7th December 2013
Accepted 29th January 2014

DOI: 10.1039/c3md00372h

www.rsc.org/medchemcomm

Introduction

Xanthenes with various substituents on the three-membered heterocyclic ring skeleton exhibit diverse biological activities, such as antihypertensive, antioxidative, antithrombotic and anticancer activities.^{1–4}

Naturally existing xanthone analogues, including gentiackochianin **1** (Fig. 1),⁵ α-mangostin **2** and psorospermin **3**, have been identified to possess noticeable anticancer activities.^{6–8} Inspired by these natural xanthenes with an excellent antiproliferative effect, many synthetic xanthenes have been derived from modification of xanthone scaffolds.^{9,10} Bisfuranoxanthone **4**, modified from the naturally isolated psorospermin **3**, exhibited comparable anticancer activities to the natural compound **3**.¹¹ Besides, in consideration of epoxy-tethered natural xanthenes, 1,3-bisepoxyxanthone **5** was

synthesized as a topoisomerase II inhibitor with significant antiproliferative activity.^{12,13}

Vadimezan **6** was developed from xanthone-4-acetic acid (XAA),^{14,15} and has been recognized as a xanthone anticancer candidate due to its excellent experimental antitumor activity as a vascular disrupting agent that attacks the blood supply of a cancerous tumor to cause tumor regression.^{16–18} Despite a phase III failure for vadimezan **6** treating advanced non-small cell lung cancer (NSCLC) with carboplatin or paclitaxel,^{19,20} study on vadimezan **6** is continuing. Ching's group compared the activities of vadimezan analogues in murine or human cellular models to explain why clinical responses to vadimezan **6** were disappointing while the preclinical data were so encouraging, and tried to search for analogues with greater clinical potential for human use.²¹

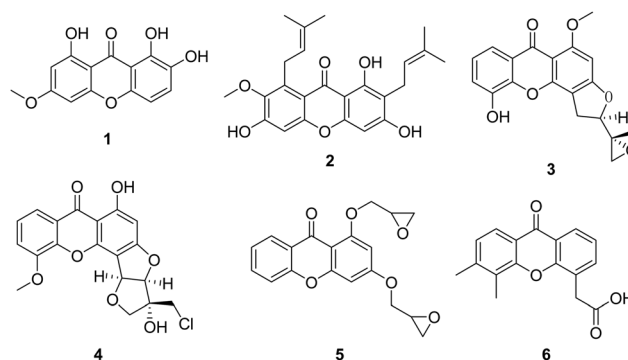


Fig. 1 Representative xanthenes with anticancer activity.

^aGraduate School, Zhejiang Chinese Medical University, Hangzhou 310053, PR China. E-mail: medchem@zcmu.edu.cn; Fax: +86-571-86613539; Tel: +86-571-86613663

^bInstitute of Biotechnology, College of Life Science, Zhejiang Chinese Medical University, Hangzhou 310053, PR China

^cR&D Center, Hangzhou Minsheng Pharmaceutical Group Co., Ltd., Hangzhou 311100, PR China

^dLaboratory of Microbiology, Nantong Center for Disease Control and Prevention, Nantong 226007, PR China

^eCollege of Pharmaceutical Science, Zhejiang University of Technology, Hangzhou 310032, PR China. E-mail: huyang@mail.hz.zj.cn; Fax: +86-571-88320557; Tel: +86-571-88320557

† Electronic supplementary information (ESI) available: Characterization data of all compounds. See DOI: 10.1039/c3md00372h

In this study we focused on the synthesis, structural characterization and preliminary evaluation of the anticancer properties of a series of new xanthone derivatives modified from vadimezan **6** with carboxyl substitution, in an attempt to further explore the therapeutic potential of this tricyclic framework.

Results and discussion

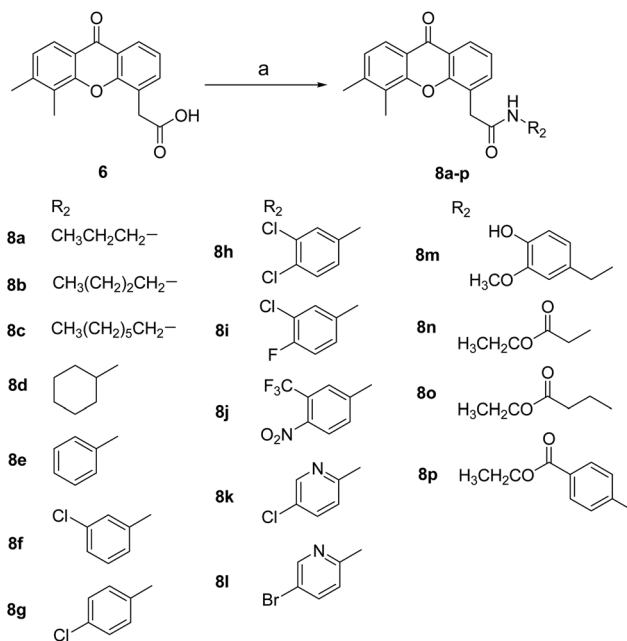
Chemistry

Vadimezan **6** was synthesized by coupling the salts of 2-hydroxyphenylacetic acid with 2-iodo-3,4-dimethylbenzoic acid, which was iodinated from the corresponding aniline with cuprous chloride and tris(2-(2-methoxyethoxy)ethyl)amine (TDA-1) catalysts to give the diacid, followed by concentrated sulfuric acid catalyzed cyclodehydration,²² with a total yield of approximately 40% and the structure was confirmed by single crystal crystallography.²³

The esters of vadimezan **6** were obtained in moderate to excellent yields with reactions of vadimezan and the corresponding alcohols catalyzed by diphenylammonium triflate (DPAT) in refluxing toluene, as shown in Scheme 1. The application of DPAT included merits from the viewpoint of green chemistry and avoided acylation of vadimezan. In addition, the products could be obtained easily by filtration after precipitation with cooling, thus simplifying the workup procedure.

Amidation of the acetic acid chain of vadimezan **6** was simply achieved by reacting with amines using *N,N'*-dicyclohexylcarbodiimide (DCC) and *N*-hydroxybenzotriazole (HOBT) under mild conditions, as shown in Scheme 2. The introduction of HOBT in the DCC coupling was beneficial in increasing the yields.

Vadimezan **6** was converted into hydrazide **9** *via* its ethyl ester **7b** by refluxing with excess hydrazine hydrate in ethanol, as shown in Scheme 3. Condensation of hydrazide **9** with the appropriate arylaldehydes afforded the corresponding arylidene hydrazides **10a–k** with *E* and *Z* conformations mixed, which

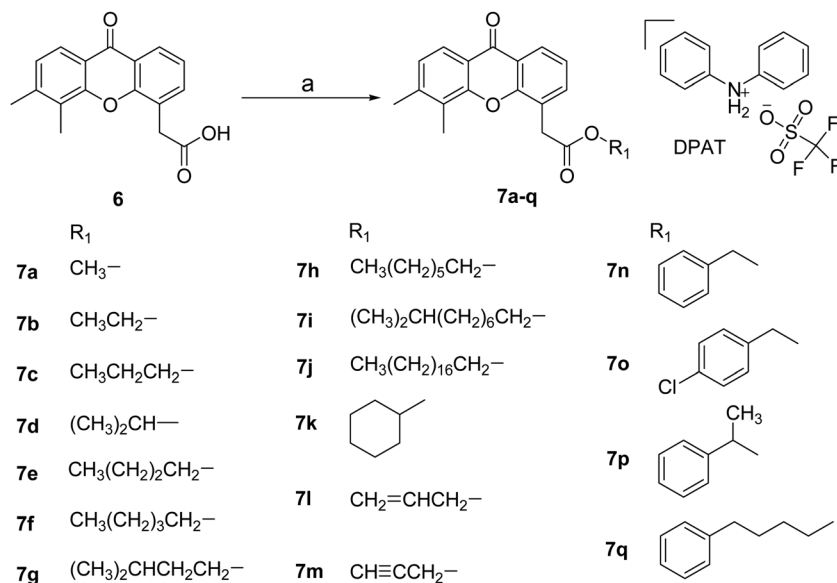


Scheme 2 Reagents and conditions: (a) R_2NH_2 , DCC, HOBT, DMF, 60 °C, 17–97%.

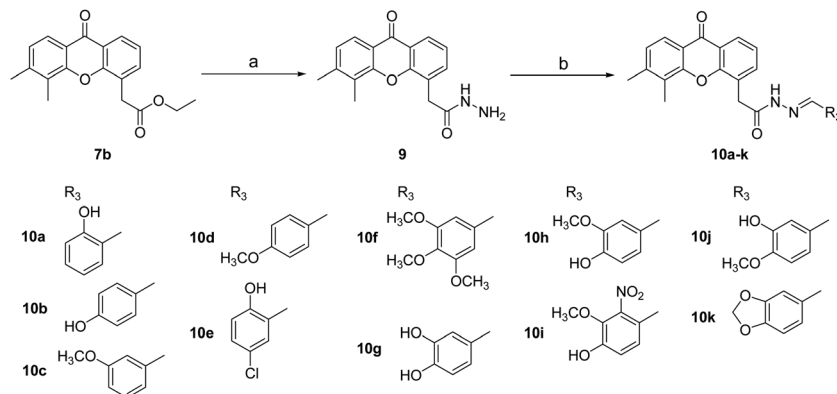
could be identified by resonance at different frequencies from 1H NMR spectra.

Hydrazide **9** was coupled with the corresponding carboxylic acids to produce diacylhydrazides of vadimezan in the presence of DCC and HOBT under mild conditions, as shown in Scheme 4. The introduction of HOBT in the DCC coupling was superior to the use of 4-dimethylaminopyridine (DMAP) in increasing the yields of diacylhydrazides **11a–c**.

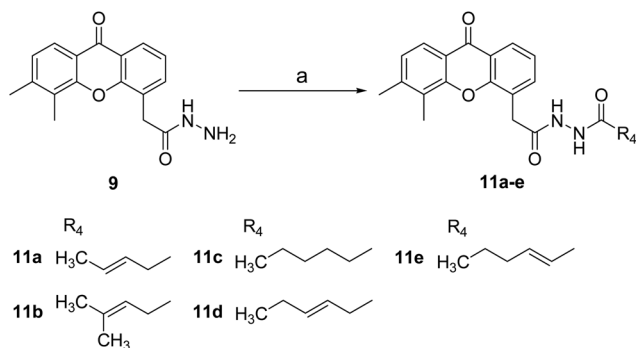
1,4-Disubstituted thiosemicarbazides **12a–c** were obtained by treating hydrazide **9** with the requisite isothiocyanates, as shown in Scheme 5.



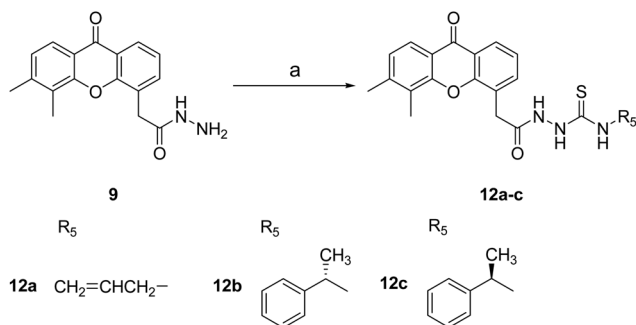
Scheme 1 Reagents and conditions: (a) R_1OH , DPAT, toluene, reflux, 27–99%.



Scheme 3 Reagents and conditions: (a) hydrazine hydrate, EtOH, reflux, 95%; (b) R_3 CHO, EtOH, reflux, 52–99%.



Scheme 4 Reagents and conditions: (a) R_4 COOH, DCC, HOBt, DMF, 50 °C, 58–98%.



Scheme 5 Reagents and conditions: (a) R_5 NCS, EtOH, reflux, 24–42%.

Pharmacology

Inhibition on cancer cell growth *in vitro*. The *in vitro* anticancer activity of vadimezan esters **7a–q** was generally weak with all IC_{50} values beyond 100 μ M, except ester **7m**, whose IC_{50} against BGC-823 was 81.5 μ M as shown in Table 1. It is thought that these esters acted as prodrugs of vadimezan **6**, which have no *in vitro* anticancer activity as reported, and could be hydrolyzed to vadimezan **6** in the body to exert the anticancer activity *in vivo*.

Compared with amides **8a**, **8b** and **8c**, there seemed a tendency that the anti-A549 activity decreased with longer side

alkyl chains of amides, but compound **8b** was most efficient against MCF-7 and HL-60 with IC_{50} at 43.8 μ M and 44.7 μ M respectively. Amide **8g** (IC_{50} = 9.4 μ M) with a *para*-chloro substituted phenyl ring was better than **8e** and 3,4-dichloro substituted **8h** in its anti-A549 activity, and comparable with *meta*-chloro **8f** (IC_{50} = 10.8 μ M), even better than combretastatin A4 (CA-4) or cisplatin (DDP). However, compound **8g** (IC_{50} = 32.1 μ M) had one-fold higher activity against the Bewo cell line as compared with **8f** (IC_{50} = 66.5 μ M). It was found that compound **8e** strongly inhibited HL-60 cells, with IC_{50} at 4.6 μ M. Besides, compounds **8k** and **8l** with pyridine substituents were not efficient against cancer cell lines, and **8k** was much weaker than **8g** in general. Vadimezan amides **8n–p** with ethyl esters of amino acids seemed to have moderate activities and their solubility was improved. The calculated partition coefficient ($\log P$) of compounds **8n** and **8o** was 3.2 and 3.4 respectively. They were predicted to have reasonable physicochemical properties of low molecular weight, $\log P$ and PSA.²⁴

Various dinitrogen compounds containing hydrazone or hydrazide subunits in their structure have been reported as interesting human cancer inhibitors.²⁵ The combination of the xanthone nucleus with a 1-hydrazinyl-2-ylidene ($-\text{NH}-\text{N}=\text{C}$) side chain might be an intriguing pharmacophore for anticancer design. Our results for the *in vitro* anticancer activity of arylidene hydrazides **10a–k** against A549 are in agreement with the prior understanding. The anticancer activity of compounds **10g–i** including *para*-hydroxyl substituents was greater than 100 μ M against A549, except compound **10b** with mono *para*-hydroxyl substitution with IC_{50} at 35.9 μ M. Comparison of the IC_{50} values between compounds **10j** and **10d**, **10j** and **10g**, respectively, showed that *meta*-hydroxyl and *para*-methoxyl groups might be crucial to maintain anti-A549 activity. Among these arylidene hydrazides, compound **10e** seemed to be the best against these cancer cells, with IC_{50} at 68.4 μ M against Ishikawa, 11.5 μ M against A549, 76.39 μ M against Bewo, 36.2 μ M against HeLa, and 20.8 μ M against HL-60.

In addition, the anticancer activity of some compounds (**7m**, **10a**, **10e**, **11a–c** and **11e**) against Jeko-1 and SK-BR-3 was further tested, and the preliminary results indicated that all their IC_{50} values were beyond 10 μ g mL⁻¹.

Table 1 IC₅₀ values of selected compounds against cancer cell lines^a (μM)

Compound	Ishikawa	A549	Bewo	HeLa	Siha	MCF-7	HL-60	BEL-7402	NCI-460	BGC-823
7m	>100	>100	>100	>100	>100	>100	>100	>100	>100	81.48
8a	>100	28.88	>100	>100	91.99	>100	>100	>100	>100	>100
8b	>100	46.86	>100	>100	>100	43.77	44.72	nt	nt	nt
8e	>100	77.56	>100	>100	>100	>100	4.59	>100	>100	>100
8f	>100	10.82	66.45	25.44	36.09	>100	91.23	nt	nt	nt
8g	>100	9.39	32.05	>100	46.65	>100	67.58	nt	nt	nt
8h	>100	92.00	>100	18.72	96.13	>100	42.44	nt	nt	nt
8i	>100	25.79	>100	94.23	32.35	>100	76.13	nt	nt	nt
8j	>100	>100	>100	>100	63.24	>100	93.77	nt	nt	nt
8k	>100	>100	>100	>100	>100	95.94	80.87	nt	nt	nt
8n	61.87	42.92	>100	>100	>100	46.38	>100	nt	nt	nt
8o	>100	35.00	26.22	>100	98.03	40.61	79.86	>100	>100	76.42
8p	>100	39.56	45.45	>100	>100	>100	90.86	>100	>100	>100
10a	>100	21.35	67.15	>100	>100	>100	52.79	>100	>100	>100
10b	>100	35.91	73.70	>100	>100	>100	>100	nt	nt	nt
10c	>100	50.74	84.86	>100	>100	>100	>100	>100	>100	>100
10d	91.16	>100	>100	>100	>100	>100	>100	nt	nt	nt
10e	68.41	11.52	76.39	36.22	>100	>100	20.83	>100	>100	>100
10f	>100	15.66	>100	>100	>100	>100	>100	nt	nt	nt
10j	>100	54.94	>100	>100	>100	>100	>100	>100	>100	>100
10k	>100	86.78	>100	>100	>100	>100	>100	>100	>100	>100
6	>100	>100	>100	>100	>100	>100	>100	>100	>100	>100
CA-4	20.10	12.52	12.74	14.83	>100	25.51	<0.03	nt	nt	nt
DDP	16.03	15.59	41.85	8.90	44.55	18.73	21.46	16.86	8.90	9.43

^a Values presented are means of three experiments; compounds with IC₅₀ larger than 100 μM against all tested cell lines are not listed; nt = not tested.

An overall view of the obtained results shows that amides **8a–p** and arylidene hydrazides **10a–k** were most active, and that the introduction of esters as **7a–q**, diacylhydrazides as **11a–e** or acyl thiosemicarbazides as **12a–c** did not seem to significantly increase the *in vitro* activity. No enantioselectivity was observed from comparison of enantiomers **12b** and **12c**.

Inhibition on HUVEC growth and migration *in vitro*. Although angiogenesis is a complex process, tube formation and cell migration are critical for endothelial cells in the organization of new blood capillaries in tumors. Compounds **8e–h** and **10e** showing the best *in vitro* anticancer activity were further evaluated for their antiangiogenic effects by tube formation assay, and vadimezan **6** was included in the assay for comparison. Tube formation assay was performed at non-cytotoxic doses of each compound against the human vein umbilical cell line (HUVEC). To identify non-cytotoxic doses for tube

formation assay, the *in vitro* cytotoxicity of selected compounds against HUVEC was assayed by MTT. The IC₅₀ values of selected compounds against HUVEC are listed in Table 2. The dose–response curves of HUVEC inhibition with the tested compounds are demonstrated in Fig. 2, indicating a linear increase in the HUVEC inhibition rate in a concentration-dependent manner; compounds **8g** and **8h** were most active and **8f** seemed weaker.

The morphological changes in HUVEC cells treated with compounds **8f–h** at 12.5 μg mL⁻¹ for 24 h were photographed as shown in Fig. 3. Compared with the control, compounds **8g** and

Table 2 IC₅₀ values of selected compounds against HUVEC^a (μM)

Compound	HUVEC inhibition
8e	>20
8f	11.10 ± 2.54
8g	6.87 ± 1.24
8h	6.40 ± 2.21
10e	>20
6	>20

^a Values presented are means ± SD.

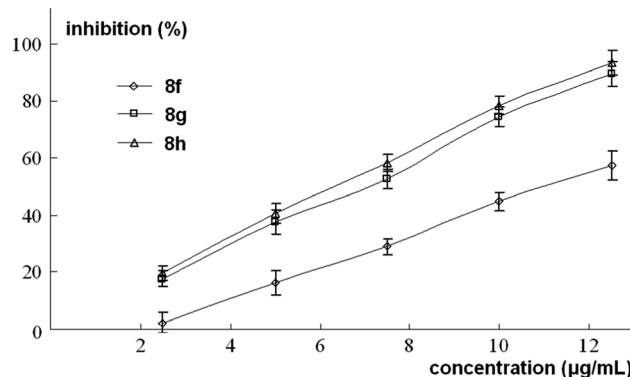


Fig. 2 Dose–response curves of HUVEC inhibition with test compounds **8f–h**.

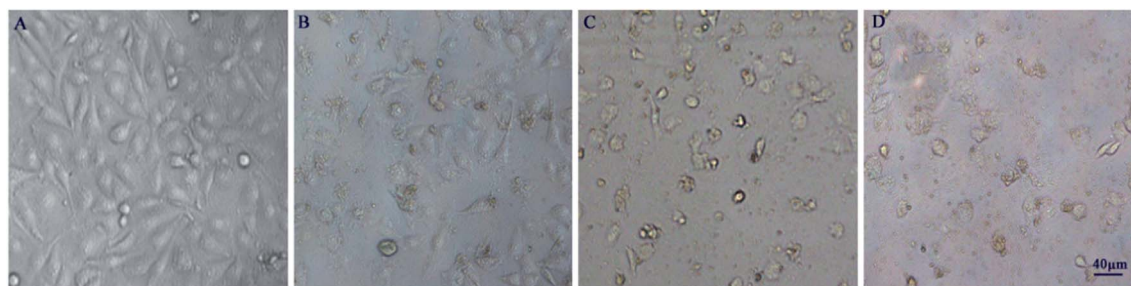


Fig. 3 Morphological changes in HUVEC cells (A) control, 24 h; (B) treated with **8f** ($12.5 \mu\text{g mL}^{-1}$), 24 h; (C) treated with **8g** ($12.5 \mu\text{g mL}^{-1}$), 24 h; (D) treated with **8h** ($12.5 \mu\text{g mL}^{-1}$), 24 h.

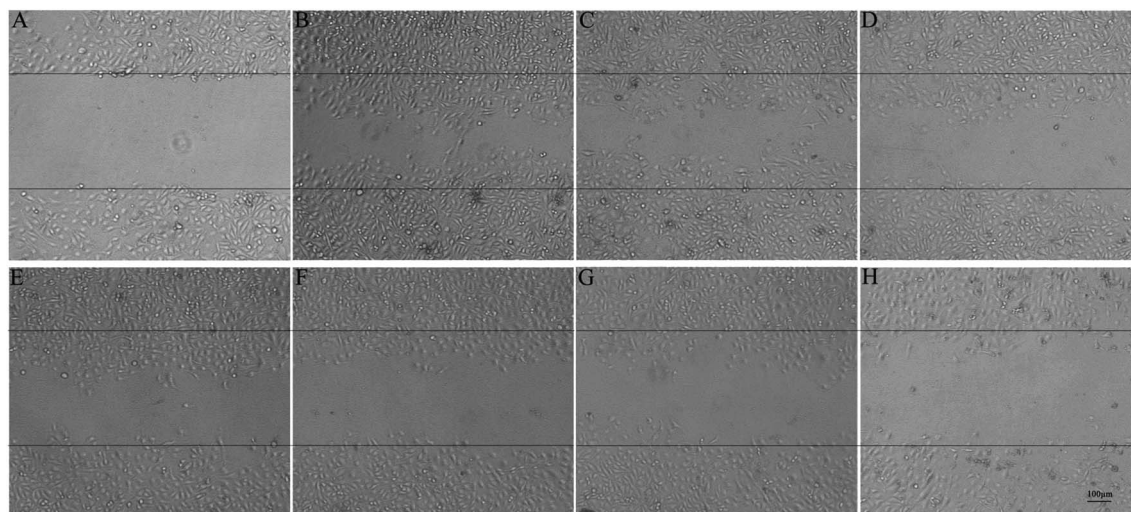


Fig. 4 Effect of **8f-h** on HUVEC cell migration (A) control, 0 h; (B) control, 24 h; (C) treated with **8f** ($2.5 \mu\text{g mL}^{-1}$), 24 h; (D) treated with **8f** ($10 \mu\text{g mL}^{-1}$), 24 h; (E) treated with **8g** ($2.5 \mu\text{g mL}^{-1}$), 24 h; (F) treated with **8g** ($10 \mu\text{g mL}^{-1}$), 24 h; (G) treated with **8h** ($2.5 \mu\text{g mL}^{-1}$), 24 h; (H) treated with **8h** ($10 \mu\text{g mL}^{-1}$), 24 h.

8h significantly changed the configuration of HUVEC cells, while vadimezan **6** at less than $500 \mu\text{M}$ (*i.e.* $141 \mu\text{g mL}^{-1}$) did not induce any morphological change in HUVEC cells as Kim's group reported,²⁶ suggesting that these derivatives of vadimezan might have a different mechanism of action at the molecular level.

The effect of compounds **8f-h** on HUVEC migration was measured by the wound healing migration assay. As shown in Fig. 4, there was a significant reduction in the ability of **8h** ($10 \mu\text{g mL}^{-1}$) treated cells to migrate into the empty space. The migration rate (%) is listed in Table 3, showing that the inhibitory effect of **8h** on HUVEC migration was 89.7% at $10 \mu\text{g mL}^{-1}$. Even at $2.5 \mu\text{g mL}^{-1}$, the reduction in migration of **8h** treated HUVEC cells was comparable to that of **8g** treated HUVEC cells at $10 \mu\text{g mL}^{-1}$. These observations indicated that these compounds, especially **8h**, could block *in vitro* angiogenesis by inhibiting endothelial cell migration.

In silico molecular docking. Buchanan *et al.* found that vadimezan **6** was a multi-kinase inhibitor targeting vascular endothelial growth factor receptor 2 (VEGFR2) in particular with an IC_{50} value at $11 \mu\text{M}$, which may contribute to the effect of vadimezan **6** on the vasculature.²⁷ Further docking studies into

Table 3 Inhibition of HUVEC cell migration treated with **8f-h**^a

Compound	Concentration ($\mu\text{g mL}^{-1}$)	Migration inhibition (%)
8f	2.5	32.58 ± 8.68
	10	58.25 ± 6.47
8g	2.5	45.62 ± 9.66
	10	65.85 ± 10.21
8h	2.5	67.58 ± 6.58
	10	89.68 ± 11.25

^a Values presented are means \pm SD.

the VEGFR2 kinase domain revealed a possible hydrogen bond between the central carbonyl group of vadimezan **6** and the backbone amide of CYS⁹¹⁹ in the inter-lobe linker region of the kinase domain. Knowing that compound **8h** exhibited anti-angiogenic activity, docking study of **8h** into the ATP binding site of VEGFR2 and EGFR was performed using AutoDock 4.0 to stimulate a binding model, based on a Lamarckian genetic algorithm (LGA) method.^{28,29} The VEGFR2 model was derived from the crystal structure of a pyridyl-pyrimidine benzimidazole bound VEGFR2 obtained from RCSB (PDB : 3EWH).³⁰ The

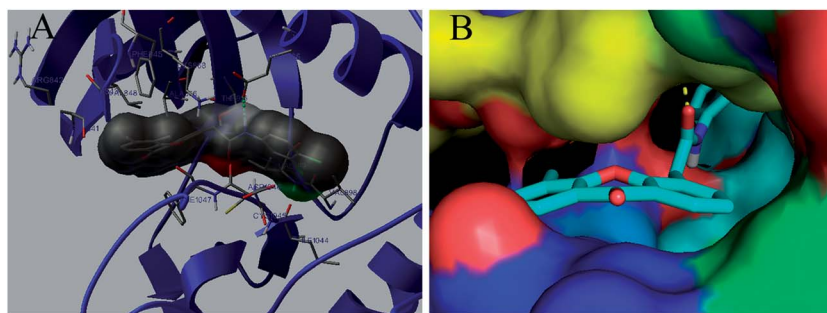


Fig. 5 (A) Binding model of **8h** with VEGFR2 displaying the interacted amino acid residue; (B) docking model of **8h** in the kinase domain of VEGFR2.

Table 4 *In vivo* antitumor efficacy of compounds against the S180 xenograft in mice^a

Group	Dose (mg kg ⁻¹)	AR ^b	No. of animals ^c	BW ^d (g)	BWL ^e (%)	TW ^f (g)	TWI ^g (%)
Control	/	Ig	11	31.77 ± 2.02	/	2.23 ± 0.41	/
6	30	Ig	7	21.84 ± 4.97**	31.25	0.53 ± 0.22**	76.23
7b	200	Ig	7	29.07 ± 3.57	8.50	2.14 ± 0.36	4.04
8a	200	Ig	7	28.49 ± 2.91*	10.32	1.66 ± 0.42*	25.56
8e	200	Ig	7	28.53 ± 2.32**	10.20	1.82 ± 0.57	18.39
8f	200	Ig	7	28.37 ± 2.64*	10.70	1.73 ± 0.37*	22.42
8g	200	Ig	7	27.84 ± 2.17*	12.37	1.61 ± 0.48*	27.80
8h	200	Ig	7	27.68 ± 3.21*	12.87	1.57 ± 0.53*	29.60

^a Values presented are means ± SD. Statistical analysis: Student's *t*-test. **p* < 0.05 vs. control, ***p* < 0.01 vs. control. ^b Administration route. ^c Number of mice tested in the group. ^d Average body weight after drug treatment. ^e Percentage of mice body weight loss vs. control group, BWL% = 100 – (mean BW_{treated}/mean BW_{control} × 100). ^f Average tumor-weight after drug treatment. ^g Percentage of tumor-weight inhibition vs. the control group, TWI% = 100 – (mean TW_{treated}/mean TW_{control} × 100).

docking results as shown in Fig. 5 indicated that compound **8h** penetrated through the Asp–Glu channel and extended to the backpocket of VEGFR2. In addition to hydrophobic interaction, compound **8h** was also involved in hydrogen bond interaction with GLU⁸⁸⁵ and the distance of the hydrogen bond was 3.03 Å. Compound **8h** displayed a total binding energy value of –10.4 kcal mol⁻¹. However, under this minimum energy conformation docking pose, hydrogen bonding between **8h** and CYS⁹¹⁹ was not observed, and the distance between the central carbonyl group of **8h** and the backbone amide of the CYS⁹¹⁹ residue was calculated to be 7.2 Å.

The EGFR model derived from the crystal structure of erlotinib bound EGFR obtained from RCSB (PDB : 1M17)³¹ was also applied to dock with **8h**, which partially occupied the ATP binding pocket of EGFR. Further *in vitro* tyrosine kinase inhibition assay was undertaken.

***In vivo* xenograft inhibition.** The *in vivo* antitumor efficacy of xanthenes was also evaluated against the S180 xenograft model in comparison with vadimezan **6** and 0.9% saline solution used as a blank control. The results presented in Table 4 showed that compounds **8a**, **8f**, **8g** and **8h** with an intragastric (ig) administration route of 200 mg kg⁻¹ of body weight once daily for consecutive six days exhibited moderate experimental therapeutic efficacy of 25.6%, 22.4%, 27.8% and 29.6%, respectively, and compound **7b** showed no significant suppression of S180 tumor growth, unlike the prodrug rationale. None of the compounds showed superior potency to vadimezan **6**,

which demonstrated 76.1% suppression of tumor growth at 30 mg kg⁻¹.

Conclusion

In order to find vadimezan derivatives with potential anti-cancer activity, a series of xanthone analogues modified from vadimezan **6** with carboxyl substitution were synthesized as esters, amides, arylidene hydrazides, diacylhydrazides and acyl thiosemicarbazides, and their *in vitro* anticancer activities were screened across a broad range of cancer cell lines. Compounds **8f**, **8g** and **10e** were most effective against A549 with IC₅₀ at 10.8 μM, 9.4 μM and 11.5 μM respectively, and **8e** with IC₅₀ at 4.6 μM against HL-60. Compounds **8f–h** showed a significant inhibitory effect on *in vitro* HUVEC growth and migration, among which **8h** inhibited HUVEC growth with IC₅₀ at 6.4 μM and HUVEC migration by 67.6% and 89.7% at 2.5 μg mL⁻¹ and 10 μg mL⁻¹, respectively. More interestingly, docking study indicated that compound **8h** might target the ATP binding site of VEGFR2. In addition, compounds **8a**, **8f–h** exhibited moderate *in vivo* antitumor efficacy against the S180 xenograft in ICR mice by 22.4–29.6% tumor weight inhibition. The results extend the previous understanding of this class of compounds, confirm the possibility for modification on the carboxylic acid group, and may help further design xanthone derivatives.

Experimental section

Chemistry

Full details about the instruments and reagents used are given in the electronic supplementary information (ESI†) along with characterization data for all compounds. Given below are protocols for the synthesis of representative compounds.

Methyl 2-(5,6-dimethyl-9-oxo-9H-xanthen-4-yl)acetate (7a). Vadimezan **6** (141 mg, 0.5 mmol), methanol (32 mg, 1.0 mmol) and DPAT (32 mg, 0.1 mmol) in toluene (15 mL) were heated to reflux for 2 h. Evaporation of the solvent under reduced pressure gave a crude product, which was purified by recrystallization from ethanol to give **7a** as a white solid, 146 mg (yield: 98.6%); Mp: 188–189 °C; IR ν_{\max} (KBr)/ cm^{-1} : 2952, 1736, 1651, 1601, 1414, 1333, 1226, 1173, 771; $^1\text{H NMR}$ (CDCl_3 , 500 MHz) δ : 8.29 (dd, $J_1 = 1.5$ Hz, $J_2 = 8.0$ Hz, 1H, Ar-H1), 8.09 (d, $J = 8.0$ Hz, 1H, Ar-H8), 7.64 (dd, $J_1 = 1.3$ Hz, $J_2 = 7.3$ Hz, 1H, Ar-H3), 7.35 (t, $J = 7.5$ Hz, 1H, Ar-H2), 7.21 (d, $J = 8.0$ Hz, 1H, Ar-H7), 4.00 (s, 2H, Ar-CH₂), 3.74 (s, 3H, OCH₃), 2.46 (s, 3H, Ar-CH₃), 2.45 (s, 3H, Ar-CH₃); EI-MS m/z (%): 296 (M^+ , 61), 238 (18), 237 (100), 236 (45), 209 (26), 165 (20).

Compounds **7b–7q** were prepared by using the same procedure for **7a**, with the corresponding alcohols.

2-(5,6-Dimethyl-9-oxo-9H-xanthen-4-yl)-N-propylacetamide (8a). Vadimezan **6** (141 mg, 0.5 mmol), DCC (124 mg, 0.6 mmol), HOBT (81 mg, 0.6 mmol) and propan-1-amine (36 mg, 0.6 mmol) were heated to 60 °C in DMF (20 mL) for 24 h, and the mixture was cooled to room temperature overnight to precipitate DCU. After filtration, the filtrate was poured into ice-water to precipitate a white solid. The crude product was collected by filtration and recrystallized from ethanol to afford compound **8a** as a white solid, 105 mg (yield: 64.9%); Mp: 187–188 °C; P_{HPLC} 96.9%, $t_{\text{R}} = 3.94$ min, ($\text{CH}_3\text{CN} : \text{H}_2\text{O} = 8 : 2$, $T_{\text{f}} = 1.0$, $\lambda = 240$ nm); IR ν_{\max} (KBr)/ cm^{-1} : 3292, 2962, 1653, 1602, 1413, 1332, 1212, 763; $^1\text{H NMR}$ (CDCl_3 , 500 MHz) δ : 8.31 (d, $J = 8.0$ Hz, 1H, Ar-H1), 8.10 (d, $J = 8.0$ Hz, 1H, Ar-H8), 7.69 (d, $J = 6.0$ Hz, 1H, Ar-H3), 7.38 (t, $J = 7.0$ Hz, 1H, Ar-H2), 7.23 (d, $J = 8.0$ Hz, 1H, Ar-H7), 5.53 (br, 1H, NH), 3.95 (s, 2H, Ar-CH₂), 3.23–3.19 (m, 2H, NHCH₂), 2.47 (s, 6H, 2 \times Ar-CH₃), 1.47–1.43 (m, 2H, CH₂CH₃), 0.80 (t, $J = 7.3$ Hz, 3H, CH₂CH₃); EI-MS m/z (%): 323 (M^+ , 29), 239 (18), 238 (100), 237 (11), 223 (18), 209 (11), 195 (11), 165 (9); anal. calcd for $\text{C}_{20}\text{H}_{21}\text{NO}_3$: C, 74.28; H, 6.55; N, 4.33%; found: C, 74.39; H, 6.61; N, 4.29%.

Compounds **8b–8p** were prepared by using the same procedure for **8a**, with the corresponding amines.

2-(5,6-Dimethyl-9-oxo-9H-xanthen-4-yl)acetohydrazide (9). A mixture of ethyl 2-(5,6-dimethyl-9-oxo-9H-xanthen-4-yl)acetate **7b** (155 mg, 0.5 mmol), ethanol (10 mL) and 85% hydrazine hydrate (2.3 mL) was refluxed for 24 h, and more hydrazine hydrate was added if necessary to reach completion. The mixture was cooled and filtered to give compound **9** as a white solid, 140 mg (yield: 94.6%); Mp: 239–241 °C; IR ν_{\max} (KBr)/ cm^{-1} : 3290, 3063, 2915, 1654, 1639, 1618, 1602, 1413, 1332, 1228, 758; $^1\text{H NMR}$ ($\text{DMSO}-d_6$, 500 MHz) δ : 9.34 (s, 1H, NHNH₂), 8.08 (dd, $J_1 = 1.5$ Hz, $J_2 = 8.0$ Hz, 1H, Ar-H1), 7.93 (d, $J = 8.0$ Hz, 1H, Ar-H8), 7.77 (d, $J = 6.5$ Hz, 1H, Ar-H3), 7.41 (t, $J = 7.5$ Hz, 1H,

Ar-H2), 7.31 (d, $J = 8.0$ Hz, 1H, Ar-H7), 4.27 (s, 2H, NHNH₂), 3.82 (s, 2H, Ar-CH₂), 2.450 (s, 3H, Ar-CH₃), 2.446 (s, 3H, Ar-CH₃); EI-MS m/z (%): 296 (M^+ , 53), 265 (72), 237 (100), 209 (10), 194 (6), 178 (6), 165 (17), 152 (4); anal. calcd for $\text{C}_{17}\text{H}_{16}\text{N}_2\text{O}_3$: C, 68.91; H, 5.44; N, 9.45%; found: C, 68.83; H, 5.38; N, 9.61%.

N'-(2-Hydroxybenzylidene)-2-(5,6-dimethyl-9-oxo-9H-xanthen-4-yl)acetohydrazide (10a). A mixture of 2-(5,6-dimethyl-9-oxo-9H-xanthen-4-yl)acetohydrazide **9** (44 mg, 0.15 mmol) and 2-hydroxybenzaldehyde (20 mg, 0.165 mmol) in ethanol (20 mL) was refluxed for 6 h. The reaction mixture was cooled and the precipitated solid was filtered, dried and recrystallized from ethanol to give compound **10a** as a white solid, 59 mg (yield: 99.2%); Mp: 247–249 °C; IR ν_{\max} (KBr)/ cm^{-1} : 3247, 3031, 1688, 1639, 1620, 1490, 1414, 1273, 1226, 752; $^1\text{H NMR}$ ($\text{DMSO}-d_6$, 400 MHz) δ : 12.03 and 11.54 (both s, total 1H, NH), 11.10 and 10.12 (both s, total 1H, OH), 8.47 and 8.37 (both s, total 1H, N=CH), 8.11 and 8.09 (both d, $J = 8.8$ Hz, total 1H, Ar-H1), 7.93 (d, $J = 8.0$ Hz, 1H, Ar-H8), 7.84 and 7.83 (both d, $J = 6.5$ Hz, total 1H, Ar-H3), 7.69 and 7.54 (both d, $J = 7.6$ Hz, total 1H, Ar'), 7.45 and 7.43 (both t, $J = 7.6$ Hz, total 1H, Ar-H2), 7.30–7.23 (m*, 1H + 1H, Ar-H7 + Ar'), 6.91 and 6.77 (both t, $J = 7.5$ Hz, total 2H, Ar'), 4.40 and 4.03 (both s, total 2H, Ar-CH₂), 2.44, 2.40, 2.39 and 2.33 (all s, total 6H, 2 \times Ar-CH₃) *overlap; EI-MS m/z (%): 400 (M^+ , 28), 296 (11), 281 (9), 265 (30), 238 (100), 209 (15), 194 (9), 165 (28); anal. calcd for $\text{C}_{24}\text{H}_{20}\text{N}_2\text{O}_4$: C, 71.99; H, 5.03; N, 7.00%; found: C, 71.86; H, 4.97; N, 7.11%.

Compounds **10b–10k** were prepared by using the same procedure for **10a**, with the corresponding aldehydes.

(E)-N'-Pent-3-enoyl-N-2-(5,6-dimethyl-9-oxo-9H-xanthen-4-yl)acetohydrazide (11a). Hydrazide **9** (44.4 mg, 0.15 mmol), DCC (37.1 mg, 0.18 mmol), HOBT (24.3 mg, 0.18 mmol) and (E)-pent-3-enoic acid (15.0 mg, 0.15 mmol) were heated to 50 °C in DMF (15 mL) for 12 h, and the mixture was cooled overnight to precipitate DCU. After filtration, the filtrate was poured into ice-water to precipitate a white solid. The crude product was collected by filtration and recrystallized from ethanol to afford compound **11a** as a pale white solid, 55.8 mg (yield: 98.4%); Mp: 187–190 °C; IR ν_{\max} (KBr)/ cm^{-1} : 3327, 2928, 2851, 1627, 1602, 1576, 763; $^1\text{H NMR}$ ($\text{DMSO}-d_6$, 400 MHz) δ : 10.17 (d, $J = 1.6$ Hz, 1H, NH), 9.86 (d, $J = 1.6$ Hz, 1H, NH), 8.08 (dd, $J_1 = 1.2$ Hz, $J_2 = 8.0$ Hz, 1H, Ar-H1), 7.92 (d, $J = 8.4$ Hz, 1H, Ar-H8), 7.83 (d, $J = 7.0$ Hz, 1H, Ar-H3), 7.42 (t, $J = 7.6$ Hz, 1H, Ar-H2), 7.30 (d, $J = 8.4$ Hz, 1H, Ar-H7), 5.58–5.43 (m, 2H, CH=CH), 3.92 (s, 2H, Ar-CH₂), 2.83 (d, $J = 6.0$ Hz, 2H, COCH₂), 2.46 (s, 3H, Ar-CH₃), 2.44 (s, 3H, Ar-CH₃), 1.60 (d, $J = 6.0$ Hz, 3H, CH₃); EI-MS m/z (%): 378 (M^+ , 65), 323 (11), 296 (49), 265 (100), 237 (100), 209 (20), 194 (11), 165 (31); EI-HRMS: M^+ 378.1587 for $\text{C}_{22}\text{H}_{22}\text{N}_2\text{O}_4$ (calcd 378.1580).

Compounds **11b–11e** were prepared by using the same procedure for **11a**, with the corresponding acids.

4-Allyl-1-(2-(5,6-dimethyl-9-oxo-9H-xanthen-4-yl)acetyl)thiosemicarbazide (12a). A mixture of 2-(5,6-dimethyl-9-oxo-9H-xanthen-4-yl)acetohydrazide **9** (59 mg, 0.2 mmol) and 3-isothiocyanatoprop-1-ene (20 mg, 0.2 mmol) in ethanol (10 mL) was refluxed for 12 h. The mixture was cooled and the precipitated solid was filtered, dried and recrystallized from ethanol to give compound **12a** as a white solid, 19 mg (yield: 24.1%); Mp:

167–170 °C; IR ν_{\max} (KBr)/ cm^{-1} : 3250, 3068, 2973, 1698, 1644, 1601, 1542, 1494, 1414, 1336, 1215, 763; ^1H NMR (DMSO- d_6 , 500 MHz) δ : 10.11 (brs, 1H, C(O)NHNH), 9.39 (s, 1H, C(O)NHNH), 8.13 (brs, 1H, C(S)NH), 8.10 (dd, $J_1 = 2.0$ Hz, $J_2 = 8.0$ Hz, 1H, Ar-H1), 7.94 (d, $J = 8.0$ Hz, 1H, Ar-H8), 7.81 (d, $J = 7.0$ Hz, 1H, Ar-H3), 7.43 (t, $J = 7.5$ Hz, 1H, Ar-H2), 7.32 (d, $J = 8.5$ Hz, 1H, Ar-H7), 5.87–5.79 (m, 1H, $\text{CH}_2\text{CH}=\text{CH}_2$), 5.14 (dd, $J_1 = 1.5$ Hz, $J_2 = 17.5$ Hz, 1H, =CHH, *cis*), 5.06 (dd, $J_1 = 1.0$ Hz, $J_2 = 10.0$ Hz, 1H, =CHH, *trans*), 4.13–4.09 (brs, 2H, $\text{CH}_2\text{CH}=\text{CH}_2$), 3.97 (s, 1H, Ar-CHH), 3.96 (s, 1H, Ar-CHH), 2.48 (s, 3H, Ar- CH_3), 2.46 (s, 3H, Ar- CH_3); EI-MS m/z (%): 384 ($[\text{M} - \text{C} + \text{H}]^+$, 3), 368 (3), 353 (2), 339 (1), 296 (14), 265 (21), 256 (15), 237 (36); ESI-HRMS: $[\text{M} - \text{H}]^-$ 394.1229 for $\text{C}_{21}\text{H}_{21}\text{N}_3\text{O}_3\text{S}-\text{H}$ (calcd 394.1225).

Compounds **12b** and **12c** were prepared by using the same procedure for **12a**, with the corresponding isothiocyanates.

Pharmacology

Cancer cell lines endometrial Ishikawa, lung A549 and NCI-460, chorion Bewo, cervical HeLa and Siha, breast MCF-7 and SK-BR-3, leukemia HL-60, liver BEL-7402, stomach BGC-823 and lymphomas Jeko-1 were obtained from Shanghai Institutes for Biological Science of the Chinese Academy of Sciences. S180 cells were provided by the Zhejiang Academy of Medical Science. ICR mice were provided by the Zhejiang Center of Laboratory Animals, male, 18–22 g, and acclimated to the laboratory environment at 25 °C prior to experimentation with food and water *ad libitum*. All animal experiments were performed in compliance with the relevant laws and institutional guidelines, and approved by the committee on animal research at the Hangzhou Minsheng Pharmaceutical Group.

Cell cultures. DMEM and RPMI1640 were purchased from Gibco, and MTT from Sigma. Each human cancer cell line was maintained in the standard medium and cultivated as a monolayer in DMEM supplemented with 800 (U v^{-1}) penicillin, 0.1% (w/v) streptomycin and 10% (v/v) fetal bovine serum (FBS). Cultures were maintained at 37 °C, 5% CO_2 in a humidified atmosphere for 3–5 d. HUVEC was grown on RPMI1640 medium containing 10% (v/v) FBS.

In vitro cancer cell growth inhibition assay. Cancer cells, treated with trypsin-EDTA solution, were seeded into 96-well plates at 10^6 cells per well, incubated in a 5% CO_2 incubator at 37 °C for 24 h, and treated with compounds synthesized at different concentrations in DMSO solution. Mitochondrial metabolism was measured as a marker for cell growth by adding 10 μL per well MTT (5 mg mL^{-1} in medium) with 48 h incubation at 37 °C. Crystals formed were dissolved in 150 μL DMSO. The absorbance was determined using a microplate reader at 570 nm. The absorbance data were converted into a cell inhibition percentage, and compared with DMSO treated cells (control culture). The percentage of inhibition was calculated by the following equation: percentage inhibition = $(1 - \text{At}/\text{Ac}) \times 100$, where At and Ac represent the absorbance in treated and control cultures, respectively. The drug concentration causing 50% cell inhibition (IC_{50}) was determined by interpolation from dose-response curves.

In vitro HUVEC growth inhibition assay. HUVEC cells were seeded on 96-well plates at 2×10^4 cells per well and incubated in a 5% CO_2 incubator at 37 °C for 24 h, followed by treatment with selected compounds **6**, **8e–h**, and **10e** at concentrations of 5 μL , 10 μL , 15 μL , 20 μL , and 25 μL in DMSO solution and incubation under 5% CO_2 at 37 °C for 48 h. Mitochondrial metabolism was measured as a marker for cell growth by adding 20 μL per well MTT (5 mg mL^{-1} in medium). Crystals formed were dissolved in 150 μL of DMSO. The absorbance was determined using a microplate reader at 570 nm.

In vitro HUVEC migration inhibition assay. HUVEC cells were seeded on 24-well plates at 2×10^4 cells per well and incubated in a 5% CO_2 incubator at 37 °C until 80% of the well bottom was spread by cells. The cell layers were wounded with a 10 μL plastic pipette tip and incubated in the presence of **8f–h**. Cell migration into the wounded area was photographed at 0 and 24 h. The migration inhibitory rate was calculated by Image-Pro Plus 6.0 software.

In silico molecular docking. Molecule **8h** was taken for prediction of the 3D structure, and the energy was minimized for flexible docking. Gasteiger charges were added and nonpolar hydrogens were merged to carbon atoms by AutoDockTools (ADT 1.4.5) and converted into the pdbqt format for the docking run. The 3D structures of VEGFR2 (3EWH) and EGFR (1M17) were obtained from the Protein Data Bank at the website: <http://www.pdb.org/>. Ligands and nonreceptor atoms such as water and ions were removed, and Kollman charges were assigned and saved in the pdbqt format as the receptor file. The grid maps defining the search region in the docking process were calculated with AutoGrid and had dimensions of $40 \times 140 \times 140$ Å centered by the predefined active site of the protein. The LGA parameters were set as default values with 50 GA runs. The best affinity modes were screened by binding energy scores and analyzed by PyMol program.

In vivo xenograft inhibition assay. To initiate tumors, S180 cells (2×10^6 cells per animal) were injected subcutaneously into the right flanks of ICR male mice. Sixty mice with near average-sized tumors were randomly assigned to seven experimental groups treated with vadimezan **6** (30 mg kg^{-1} of body weight), **7b** (200 mg kg^{-1}), **8a** (200 mg kg^{-1}), **8e** (200 mg kg^{-1}), **8f** (200 mg kg^{-1}), **8g** (200 mg kg^{-1}) and **8h** (200 mg kg^{-1}), and a control group with eleven mice treated with a vehicle of 0.9% saline solution (0.1 mL/10 g of body weight) once daily through the ig administration route from the second day after establishing the mouse model for consecutive six days. The tumor bearing animals were observed everyday and euthanized after experiment and the solid tumors were weighed for calculating the tumor weight inhibition of compounds in the S180 xenograft model.

Acknowledgements

The authors thank the Center of Analysis & Measurement of Zhejiang University and College of Chemistry and Life Sciences, Zhejiang Normal University for characterization of the compounds and partial financial support. S.-J. Zhang is grateful to the research fund from the Zhejiang Chinese Medical University for financial support (2011ZY26).

Notes and references

- 1 Y. Na, *J. Pharm. Pharmacol.*, 2009, **61**, 707–712.
- 2 N. Pouli and P. Marakos, *Anti-Cancer Agents Med. Chem.*, 2009, **9**, 77–98.
- 3 M. M. M. Pinto, M. E. Sousa and M. S. J. Nascimento, *Curr. Med. Chem.*, 2005, **12**, 2517–2538.
- 4 H. R. El-Seedi, M. A. El-Barbary, D. M. H. El-Ghorab, L. Bohlin, A. K. Borg-Karlson, U. Goransson and R. Verpoorte, *Curr. Med. Chem.*, 2010, **17**, 854–901.
- 5 A. Isakovic, T. Jankovic, L. Harhaji, S. Kostic-Rajacic, Z. Nikolic, V. Vajs and V. Trajkovic, *Bioorg. Med. Chem.*, 2008, **16**, 5683–5694.
- 6 K. Matsumoto, Y. Akao, E. Kobayashi, K. Ohguchi, T. Ito, T. Tanaka, M. Iinuma and Y. Nozawa, *J. Nat. Prod.*, 2003, **66**, 1124–1127.
- 7 Y. Kwok, Q. P. Zeng and L. H. Hurley, *Proc. Natl. Acad. Sci. U. S. A.*, 1998, **95**, 13531–13536.
- 8 M. Hansen, S. J. Lee, J. M. Cassady and L. H. Hurley, *J. Am. Chem. Soc.*, 1996, **118**, 5553–5561.
- 9 S. Boutefnouchet, N. T. Minh, R. Putrus, B. Pfeiffer, S. Léonce, A. Pierré, S. Michel, F. Tillequin and M. C. Lallemand, *Eur. J. Med. Chem.*, 2010, **45**, 581–587.
- 10 S. Boutefnouchet, N. Gaboriaud-Kolar, N. T. Minh, S. Depauw, M. H. David-Cordonnier, B. Pfeiffer, S. Léonce, A. Pierré, F. Tillequin, M. C. Lallemand and S. Michel, *J. Med. Chem.*, 2008, **51**, 7287–7297.
- 11 R. A. Heald, T. S. Dexheimer, H. Vankayalapati, A. Siddiqui-Jain, L. Z. Szabo, M. C. Gleason-Guzman and L. H. Hurley, *J. Med. Chem.*, 2005, **48**, 2993–3004.
- 12 S. Woo, J. Jung, C. Lee, Y. Kwon and Y. Na, *Bioorg. Med. Chem. Lett.*, 2007, **17**, 1163–1166.
- 13 S. Woo, D. H. Kang, J. M. Nam, C. S. Lee, E. M. Ha, E. S. Lee, Y. Kwon and Y. Na, *Eur. J. Med. Chem.*, 2010, **45**, 4221–4228.
- 14 G. W. Rewcastle, G. J. Atwell, B. C. Baguley, M. Boyd, L. L. Thomsen, L. Zhuang and W. A. Denny, *J. Med. Chem.*, 1991, **34**, 2864–2870.
- 15 G. W. Rewcastle, G. J. Atwell, L. Zhuang, B. C. Baguley and W. A. Denny, *J. Med. Chem.*, 1991, **34**, 217–222.
- 16 B. C. Baguley, *Lancet Oncol.*, 2003, **4**, 141–148.
- 17 G. M. Tozer, C. Kanthou and B. C. Baguley, *Nat. Rev. Cancer*, 2005, **5**, 423–435.
- 18 J. W. Lippert, *Bioorg. Med. Chem.*, 2007, **15**, 605–615.
- 19 M. Head and M. B. Jameson, *Expert Opin. Invest. Drugs*, 2010, **19**, 295–304.
- 20 P. Lara, J. Douillard, K. Nakagawa, J. Von Powel, M. J. McKeage, I. Albert, G. Losonczy, M. Reck, D. S. Heo, X. Fan, A. Fandi and G. Scagliotti, *J. Clin. Oncol.*, 2011, **29**(15), suppl; abstr 7502.
- 21 S. M. Tijono, K. Guo, K. Henare, B. D. Palmer, L. C. S. Wang, S. M. Albelda and L. M. Ching, *Br. J. Cancer*, 2013, **108**, 1306–1315.
- 22 G. J. Atwell, S. J. Yang and W. A. Denny, *Eur. J. Med. Chem.*, 2002, **37**, 825–828.
- 23 S. J. Zhang and W. X. Hu, *Acta Crystallogr., Sect. E: Struct. Rep. Online*, 2010, **E66**, o2082–o2083.
- 24 *Molinspiration Property Engine v2011.04*, <http://www.molinspiration.com/cgi-bin/properties>, accessed on Jul. 7, 2013.
- 25 L. R. Morgan, K. Thangaraj, B. LeBlanc, A. Rodgers, L. T. Wolford, C. L. Hooper, D. Fan and B. S. Jursic, *J. Med. Chem.*, 2003, **46**, 4552–4563.
- 26 S. Kim, L. Peshkin and T. J. Mitchison, *PLoS One*, 2012, **7**, e40177.
- 27 C. M. Buchanan, J. H. Shih, J. W. Astin, G. W. Rewcastle, J. U. Flanagan, P. S. Crosier and P. R. Shepherd, *Clin. Sci.*, 2012, **122**, 449–457.
- 28 G. M. Morris, D. S. Goodsell, R. S. Halliday, R. Huey, W. E. Hart, R. K. Belew and A. J. Olson, *J. Comput. Chem.*, 1998, **19**, 1639–1662.
- 29 R. Huey, G. M. Morris, A. J. Olson and D. S. Goodsell, *J. Comput. Chem.*, 2007, **28**, 1145–1152.
- 30 V. J. Cee, A. C. Cheng, K. Romero, S. Bellon, C. Mohr, D. A. Whittington, A. Bak, J. Bready, S. Caenepeel, A. Coxon, H. L. Deak, J. Fretland, Y. Gu, B. L. Hodous, X. Huang, J. L. Kim, J. Lin, A. M. Long, H. Nguyen, P. R. Olivieri, V. F. Patel, L. Wang, Y. H. Zhou, P. Hughes and S. Geuns-Meyer, *Bioorg. Med. Chem. Lett.*, 2009, **19**, 424–427.
- 31 J. Stamos, M. X. Sliwowski and C. Eigenbrot, *J. Biol. Chem.*, 2002, **277**, 46265–46272.